Energy-optimal human walking with feedback-controlled robotic prostheses: a computational study

Matthew L. Handford and Manoj Srinivasan, *Member, IEEE*

***Abstract*—Lower limb amputees, on average, experience reduced mobility and higher metabolic rates than non-amputees. It may be possible to improve their mobility and metabolic rate with an optimized robotic prosthesis. However, we still need to determine what specific parameters we should optimize. Here, we use large-scale trajectory optimization on a simulated transtibial amputee with a robotic prosthesis to obtain metabolic energy-minimizing walking gaits with multiple prosthesis controllers. Using this simulation, we were able to obtain trends in the energetics and kinematics for various levels of prosthesis work. We find that the net metabolic rate has a roughly quadratic relationship with the net prosthesis work rate. This simulation predicts that metabolic rate could be reduced below that of a non-amputee, although such gaits are highly asymmetric and not seen in experiments with amputees. Walking simulations with left-right symmetry in kinematics or ground reaction forces have higher metabolic rates than asymmetric gaits, suggesting a potential reason for asymmetries in amputee walking. Our findings suggest that a computational framework such as the one presented here could augment the experimental approaches to prosthesis design iterations, although quantitatively accurate prediction of experiments from simulation remains an open problem.**

I. Introduction

MOST transtibial amputees experience reduced mobility and higher metabolic rates during walking, likely due to the limitations in currently available passive prostheses [1]. Such passive prostheses are incapable of producing net positive power, thus placing that burden on the amputee's unaffected joints. In contrast, robotic (active) ankle-foot prostheses can produce human levels of torque and power during a walking task with relatively little increase in mass [2], [3]. Despite these capabilities, switching from passive to active prostheses only produces a small reduction [3], [4] or no reduction [5] in metabolic rate for the average user. With such high-performance components underachieving in their purpose, the fault could be in the way the prosthesis is controlled.

Robotic lower limb prostheses are often controlled through a mixture of feedback and feedforward control. Feedback control is based on state variables such as prosthesis angle, angular rate, center of pressure, or myoelectric activity (EMG) of neighboring muscles [2], [4], [6]. Controllers with feedforward elements are usually not entirely feedforward, but have some state-based or event-based resets, such as restarting the controller at every heel-strike [7]–[9]. The parameters of such controllers are often designed and tuned with user feedback or measured kinematics or energetics [4]. Such controller tuning is sometimes formalized using 'body-in-the-loop' optimization or adaptive control frameworks [10]–[13]. To inform the design of these controllers, we could use a mathematical model to predict the consequences of different control strategies and prosthesis parameters for whole body locomotion. A well documented principle for predicting walking behavior is metabolic minimization [14]–[19]. Humans walk in a manner that minimizes their metabolic rate (approximately) [20]–[23], even when wearing prostheses [24] or moving unsteadily [25], potentially after a learning phase [26], [27]. Here, our goal is the prediction of amputee walking behavior via energy optimality, rather than tracking experimentally-obtained kinematics in able-bodied or amputee walking. Simulations with kinematic tracking have been pursued by a number of prior studies [17], [28]–[31].

In a previous study [32], we used a mathematical model of a human walking with a unilateral robotic prosthesis to consider the idealized case of the prosthesis capable of an arbitrary torque as a function of time at the ankle. The high dimensionality of the prosthesis actuation as a piecewise linear function of time allows us to discover close to the greatest possible metabolic reduction in a mathematical model. However, such an idealized calculation may only be useful as a benchmark and may not be practical for a real-world device since it produces purely time-based feedforward control for a perfectly periodic gait at a single walking speed.

Here, we attempt to predict the effects of constraining the prosthesis actuation to four simple feedback controllers: three active controllers based on ankle 'torque-angle relationships' [2], [4], [33]–[35] and one passive prosthesis based on the SACH foot [1]. Each of the three active controllers is designed with a different torque-angle loop and a single parameter which can be used to vary the amount of work being applied by the prosthesis. We examine the implications of the assumed torque-angle loop shape and test whether increasing net prosthesis work always reduces net metabolic rate. We also determine a relationship between bilateral asymmetry and net metabolic rate using these controllers both with and without bilateral symmetry constraints. Finally, we compare our simulation results with published experimental data [5].

Mechanical and Aerospace Engineering, The Ohio State University
Manuscript received DATE; revised DATE.

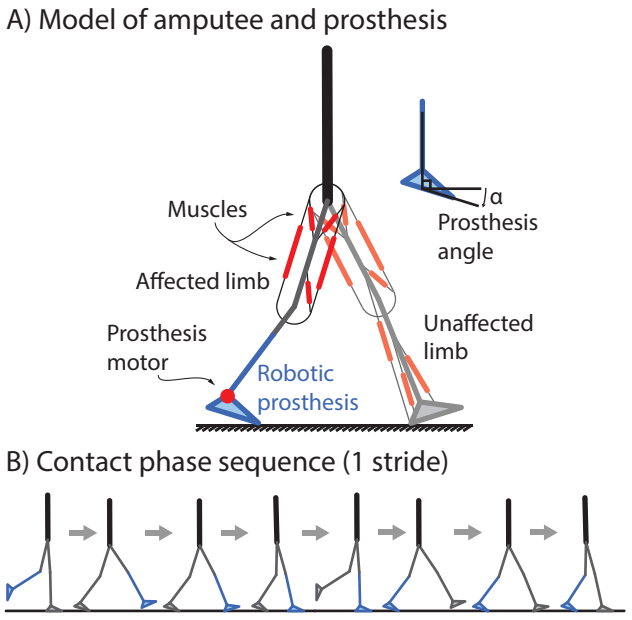

Fig. 1. **A planar model of a person with a unilateral ankle-foot prosthesis**. a) Our biped model with seven rigid body segments and thirteen uni- and biarticular muscles (eight on the unaffected limb and five on the affected side due to the amputation of the shank and foot). The prosthesis ankle joint is actuated by an electric motor (idealized as a torque source). The prosthesis ankle angle α (inset) is assumed to be positive for plantarflexion and negative for dorsiflexion. b) The sequence of contact phases during a single walking stride. The contact phases are defined by the parts of each foot (the heels and the toes) that are in contact with the ground. See [32] for more details.

II. Methods

A. Human model with a robotic prosthesis

The model we use to simulate a unilateral transtibial amputee consists of seven body segments and includes an ankle-foot prosthesis (Figure 1a). Five biological joints (two hips, two knees, and one ankle) are actuated by thirteen uni- and biarticular muscles that produce piecewise linear forces. These simplified muscles lack activation dynamics and force-length relationships common in the Hill-Type muscle model [36], but are constrained by the muscles' force-velocity relationships. The prosthesis shank is rigidly attached to the body. Thus, we ignore socket dynamics and implicitly simulate a perfect socket fit or a bone anchored pylon. The prosthetic ankle joint is actuated by an ideal torque motor with no internal motor dynamics. Muscle and body segment properties are drawn from past literature and assume a nominal 70 kg person [32], [37], [38]. The prosthetic foot is assumed to match the mass and inertia properties of the biological foot to isolate the source of any bilateral gait asymmetries to the control of the prosthesis rather than the inertial properties of the limb. Since most real world prostheses have a smaller mass and moment of inertia compared to the biological shank and foot [39]–[42], we also test the dependence of gait on prosthesis inertia by reducing the prosthesis inertial properties by 30% for some calculations. We define a full walking cycle by dividing a stride into eight 'contact phases' with different equations of motion based on which heels or toes of the unaffected limb (the intact limb with no prosthesis) and affected limb (the limb with the amputation and the prosthesis) are on the ground (as in [32] and Figure 1b here). Ground contact has no compliance: a perfectly inelastic collision occurs whenever a heel or toe contacts the ground.

B. Variable work feedback control

The prosthesis torque is determined by state feedback using prosthesis ankle angle α, angular rate $\dot{\alpha}$, and contact phase. We consider three families of torque-angle relationships during stance (Figure 2). Controller 1 (Figure 2a) is based on a simple controller used on the BioM prosthesis [4]. Controllers 2 and 3 (Figures 2b and 2c) are based on those used in prosthesis emulators by Caputo and Collins [2]. The three controller families are each parameterized by one variable, allowing us to change the area within the torque-angle work-loop, thereby changing the net prosthesis work. For a typical gait cycle, all three controllers are identical during the swing and initial stance phases, but differ in how they apply power during late stance, as described below (see Figure 2e for more detail on the various stance phases).

1) Initial stance phase control is spring-like: The 'initial stance phase' for the prosthesis starts at heel-strike, continues into the flat-foot contact phase (with both heel and toe on the ground), and then transitions into the push-off phase (defined in the next paragraph, see Figure 2e). During this initial stance phase, all three controllers act like linear torsional springs with stiffness 290 $\mathrm{N\,rad^{-1}}$, no damping, and rest angle $\alpha_{rest} = 0.062$ rad (3.5°) of plantar-flexion.

2) Three strategies for active push-off during late stance: At the onset of push-off (when ankle angular rate $\dot{\alpha}$ changes from negative to positive after the heel has left the ground), the three controllers affect the stance work of the prosthesis through three distinct strategies. Controller 1 adds a constant torque offset $\Delta\tau$ to the linear spring-like behavior during initial stance. This torque offset is achieved by changing the rest angle $\Delta\alpha_{\mathrm{rest}}$ while keeping the stiffness constant (Figure 2a). Controller 2 uses a new linear torque-angle relation by changing the rest angle $\Delta\alpha_{\mathrm{rest}}$, with the new stiffness selected so as to produce a continuous torque throughout the stance phase (Figure 2b). Controller 3 maintains the maximum torque produced when dorsiflexion ends and holds it for a specified change in prosthesis angle $\Delta\alpha_{\mathrm{rest}}$ before returning to the original stiffness (Figure 2c). Thus, each of the three controller types represents a one parameter family of controllers, parameterized by the single variable $\Delta\alpha_{\mathrm{rest}}$.

3) PD control during swing phase: During the 'prosthesis swing phase,' when the prosthesis is not in contact with the ground, all three controllers use a proportional-derivative (PD) controller. This PD controller resets the prosthetic foot rest angle to zero ($\alpha_{\mathrm{rest}} = 0$), thus re-positioning the prosthetic foot perpendicular to the shank. We use a proportional gain (torsional stiffness) of 36.25 $\mathrm{N\,rad^{-1}}$ and a derivative gain (damping) of 2.29 $\mathrm{Ns\,rad^{-1}}$. These gain values prevent under-damped foot oscillations during swing and reset the prosthesis angle in time for the next heel strike.

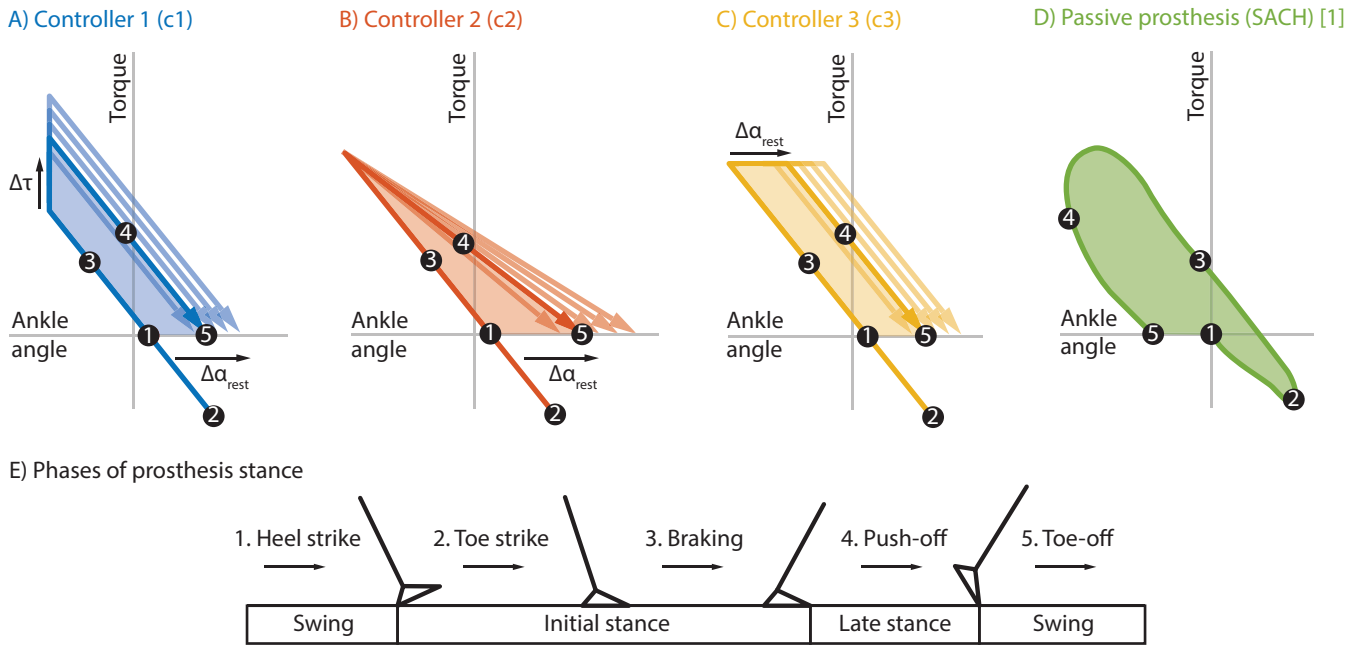

Fig. 2. **Torque-angle work-loops during stance for three prosthesis controllers.** All three controllers have the same linear spring-like behavior during initial stance (phases 1-3). They differ in how they perform net mechanical work during push-off (phase 4). A) Controller 1. Push-off work is controlled through the addition of a constant torque offset $\Delta\tau$, equivalent to increasing the rest angle by $\Delta\alpha_{\text{rest}}$ while maintaining stiffness. B) Controller 2. Push-off work is controlled through adjusting the rest angle (by $\Delta\alpha_{\text{rest}}$) and stiffness to create a continuous torque throughout stance. C) Controller 3. Push-off work is controlled through maintaining the maximum torque produced during dorsiflexion over a range of ankle angles $\Delta\alpha_{\text{rest}}$, then returns to the linear stiffness used in the initial stance phase. D) Passive controller. The work-loop shown is taken from experimental data while walking with a SACH foot [1]. E) Prosthesis stance phase sequence. Heel strike, toe strike, and braking all belong to the initial stance phase. Initial stance is followed by late stance (push-off) which lasts until the toe leaves the ground. The leg then continues into the swing phase. Numbers 1 to 5 are overlaid on panels A-D, corresponding to the prosthesis contact phases sequence shown.

C. Passive and optimal controllers for comparison

In addition to the three controllers, we also define a 'passive' controller and an 'optimized' controller for comparison. For our 'passive' controller, we simulate the SACH foot through a non-linear spring and damper system with parameters determined using linear regression on real world data [1]. For our 'optimized' controller, we allow the prosthesis torque versus time to also be an unknown calculated by the optimization (in addition to the muscle forces), identical to the procedure in a previous study [32]. As in [32], we allowed such 'arbitrary' prosthesis torque variations (within some torque bounds) and minimized a weighted sum of the human and prosthesis torque squared cost (weighted, respectively, by λ and $1-\lambda$, where $\lambda = 1$ implied optimizing only the human cost). For the results here, we used $\lambda = 0.95$, as $\lambda = 1$ caused convergence issues [32].

D. Trajectory optimization for energy-optimal walks

To predict walking kinematics and energetics, we use numerical optimization to compute the periodic walking motion that minimizes the metabolic rate over one stride (two steps) [20], [21], [32]. This gait is set to a walking speed of v_{avg} = 1.3 ms^{-1} and is subject to physiological strength, foot clearance, and range of motion constraints. The stride is divided into eight contact phases (Figure 1b), with each contact phase divided further into eight equal time segments, each with unknown initial conditions for the state variables and unknown values for the controls, namely, muscle forces and prosthesis torque. This results in a multiple shooting-like transcription of the optimization problem [43]. The values of these unknown initial conditions, piecewise linear controls, and contact phase durations are then determined by numerical optimization (using the software [44]). We enforce continuity of body state and control across all time segments and allow velocity discontinuity only at foot-ground collisions [32]. The prosthesis controllers (as specified by the torque-angle loops in Figure 2) are implemented by enforcing an appropriate equality constraint relating the prosthesis torque, angle, and angular rate.

The objective function we minimize is a combination of a modified version of a metabolic rate model $\dot{C}_{\text{met}}$ suggested by Alexander and Minetti [20], [21], [32] and a small muscle force rate cost $\dot{C}_{\text{FR}}$, summed over all muscles:

$$\dot{C}_{\text{met}} = \frac{1}{T_s}\int_0^{T_s}\left[\sum_i \left[\gamma(a_i) + a_i\phi\left(\bar{v}_i\right)\right] F_{\text{iso},i} v_{\text{max},i}\right] dt,$$

where T_s is stride duration, i represents muscle index, a_i is muscle activation, $F_{\text{iso},i}$ is maximum isometric force, and $v_{\text{max},i}$ is maximum muscle shortening velocity. The function $\gamma(a_i) = \beta\left(a_i + a_i^2\right)$ is an activation cost with $\beta = 0.05$,

and the function $\phi(\bar{v}_i)$ describes the metabolic dependence on normalized shortening velocity $\bar{v}_i = v_i/v_{\max,i}$, where v_i is muscle shortening velocity. A more detailed model description and the values used for the aforementioned parameters can be found in the main body and appendix of [32], which are based on [38]. Here, minimizing cost per unit time $\dot{C}_{\text{met}}$ is equivalent to minimizing cost per unit distance $\dot{C}_{\text{met}}/v_{\text{avg}}$ because the forward speed v_{avg} is fixed [45]. The metabolic rate used here is the 'net' metabolic rate of walking as it does not include the resting metabolic rate, instead measuring the metabolic rate of walking over and above that of standing still. To this metabolic rate function, we add a small muscle force rate cost of:

$$\dot{C}_{\text{FR}} = \frac{\alpha}{T_s}\int_0^{T_s}\left[\sum_i \dot{F}_i^2/F_{\text{iso},i}^2\right]dt,$$

where $\dot{F}_i$ is the muscle force rate and α is a small weighting coefficient equal to 5×10^{-4}. This additional small force rate term penalizes rapid force changes, avoids convergence to local minima with erratic muscle forces, but is weighted to be so small that it does not increase the optimal metabolic rate $\dot{C}_{\text{met}}$. Some prior experiments also suggest that muscle metabolic cost has such a force-rate related term [46], although we have not attempted to incorporate this term quantitatively.

E. Bilateral symmetry constraints

Optimizations using the model described above allow the two steps of the simulated stride to be different, so that the gait can have bilateral (left-right) asymmetry. We then performed a series of optimizations by including bilateral symmetry constraints. We considered four types of symmetry: symmetry in step time, symmetry in joint kinematics (angles and angular rates), symmetry in ground reaction forces (GRF), and symmetry in both kinematics and GRFs. In each case, we constrained the variables corresponding to the two limbs to be equal, except for the kinematic symmetry constraint, where we allowed the variables to differ by a maximum of 0.02 rads at any given time.

III. Results

A. Increase in prosthesis work rate reduces metabolic rate

We obtained gaits that minimized metabolic energy with the three prosthesis controllers for net prosthesis work rates $\dot{W}_{\text{pros}}$ ranging between -0.3 and 1.0 W kg^{-1}, by considering a range of rest angle changes ($\Delta\alpha_{\text{rest}}$) for the prosthesis. Specifying $\Delta\alpha_{\text{rest}}$ constrains the work approximately and not exactly. This is because, like humans, the model can vary stance time, push-off angle and push-off timing, even if the shape of the overall torque-angle-loop is constrained. As prosthesis work rate increases, there is a decrease in metabolic rate down to a minimum. Any further increase in work led to increased metabolic rate. We highlight this non-monotonic behavior in metabolic rate reduction by the quadratic fit: $\dot{C} = 2.4 - 4.0\dot{W}_{\text{pros}} + 3.2\dot{W}_{\text{pros}}^2$ (shown in Figure 3). At the optimal net prosthesis work rate, the predicted human metabolic rate due to all three controllers was about 1.0 W kg^{-1}.

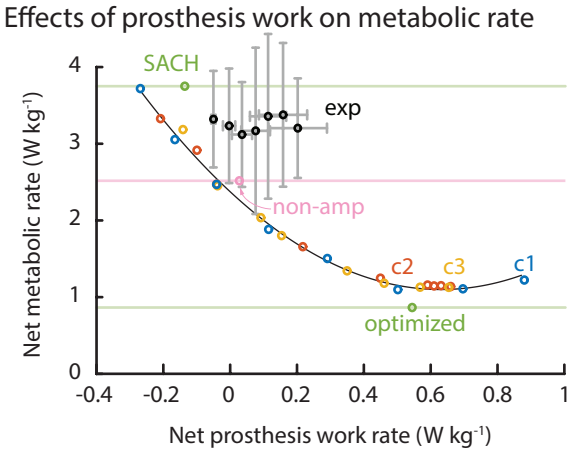

Fig. 3. **Effects of prosthesis work on metabolic rate.** For Controller 1 (c1, blue), Controller 2 (c2, red), and Controller 3 (c3, yellow), the relationship between net metabolic rate and net prosthesis work rate is non-monotonic and has a minimum. A quadratic fit to pooled data from all three controllers ($\dot{C}_{\text{met}} = 2.4 - 4.0\dot{W}_{\text{pros}} + 3.2\dot{W}_{\text{pros}}^2$) is shown. The simulated SACH foot and the optimized prosthesis controller (both shown in green) occupy two extremes. The SACH foot has high metabolic rate and low prosthesis work, whereas the optimized controller has low metabolic rate and high prosthesis work. Metabolic rate versus work rate for human subject experiments shows no systematic trend and has high variability (mean $\pm$ standard deviation, shown in black and gray) [5].

B. Simple feedback is worse than optimized control but both are better than SACH foot

As expected, the metabolic rates from using the simple feedback controllers were higher than when the prosthesis torque was optimized as an arbitrary function of time (that is, unconstrained by a simple torque-angle feedback relation). Minimizing the composite human-plus-prosthesis cost function weighted mostly toward the human metabolic rate ($\lambda = 0.95$), we find an optimal metabolic rate around 0.86 W kg^{-1}. Thus, this optimized control produces about an 14% lower metabolic rate than the torque-angle-based feedback controllers at their optimum (Figure 3). In contrast, simulating a passive prosthesis, namely, the SACH foot, we found a cost of about 3.8 W kg^{-1}, a much higher cost than all other controllers tested at similar work levels.

C. Zero work prostheses can give near-able-bodied costs

All three controllers have a zero net stance work condition, in which the controllers behave like an undamped spring and perform equal amounts of positive and negative work over a stance phase. These zero work conditions resulted in amputee metabolic rates that were comparable to our model predictions for able-bodied simulations (Figure 3). This result echoes the recent experiments in which the metabolic rates of physically active and well-trained amputees with passive energy-storage-and-return (ESR) prostheses were negligibly different from that of able-bodied controls [31], [47]. This result may also be related to the reduction of muscle work requirements in walking and running via energy storage and return in tendons, other elastic structures, or passive exoskeletons [48], [49] and the ability of simple springy-legged models to walk without actuator work [21], [50].

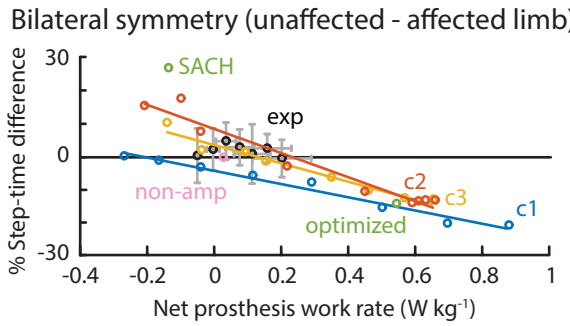

Fig. 4. **Bilateral symmetry is correlated with prosthesis work.** The bilateral symmetry, as quantified by percent step time difference (the percent of the stride time spent on the unaffected side minus the percent of stride spent on the affected side), is shown for each controller (c1, c2, c3) at various prosthesis work rates. The percent step time difference decreases, roughly linearly, with increased positive prosthesis work. Thus the biped spends more time on the affected side as the robotic prosthesis provides more net positive work rate. In contrast, a net negative prosthesis work rate generally corresponds to less time spent on the affected side. Experimental data [5] (black and gray error bars) and the simulated non-amputee result (pink circle) are shown for comparison. The SACH foot results in a highly asymmetric gait with more time spent on the unaffected limb, whereas the optimized robotic prosthesis results in large asymmetry in the opposite direction (green circles).

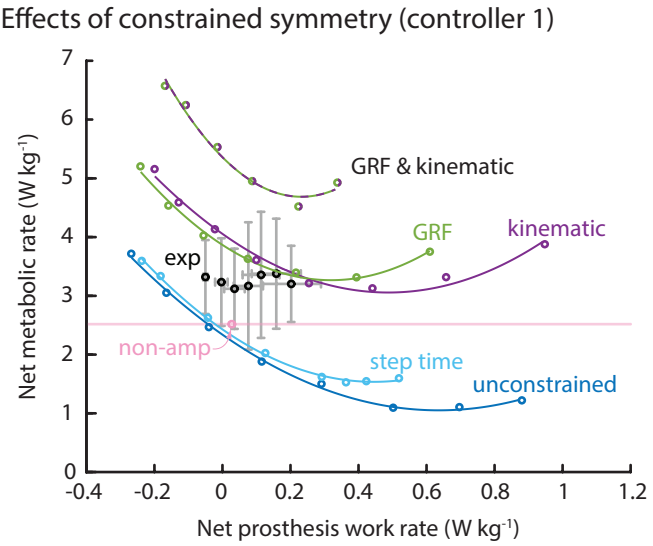

Fig. 5. **Controller 1 with various symmetry constraints.** Applying step time, kinematic, or ground reaction force (GRF) symmetry constraints to the simulation increases the metabolic rate over the unconstrained condition. When both kinematic and ground reaction force constraints are enforced, the metabolic rate is much higher than any constraint alone. Experimental metabolic data [5] (black and gray error bars) and simulated non-amputee metabolic rate (pink circle and line) are shown for comparison.

D. All energy-optimal gaits are asymmetric

When there were no explicit constraints on symmetry, all energy optimal gaits were bilaterally asymmetric. Figure 4 shows the stance time percent difference between the unaffected and affected stance times. This stance time difference is a necessary condition for symmetry but not a sufficient condition. Non-zero stance time difference implies asymmetry, but zero stance time difference admits asymmetry in other aspects of the gait. For all controllers considered, increase in net positive prosthesis work was associated with more stance time on the affected side. The optimizations predicted that walking with a SACH foot would have the opposite asymmetry, so that the person spends more time on the unaffected foot, as also seen in experiments [51], [52]. Experiments involving amputees wearing robotic prostheses [5] did not show strong correlations between symmetry and prosthesis power, whereas in other non-amputee prosthesis emulator experiments [2], the prosthesis stance fraction increased with prosthesis power, as predicted by our model.

E. Symmetry constraints increase metabolic cost but promote kinematics closer to experiment

We found that the metabolic rates increased with symmetry constraints (Figure 5). For step time symmetry, the metabolic rate increased slightly (by about 6% over the unconstrained condition at zero work). The metabolic rate increase was similar for constraining just the kinematics or the ground reaction forces (by about 60% over the unconstrained condition at zero work), but constraining symmetry in both kinematics and ground reaction forces increased the costs much more (by about 120% over the unconstrained condition at zero work). We find that the addition of the symmetry constraint improves correspondence between simulation predictions and experimental observations [5], for metabolic rates (Figure 5) joint kinematics, and joint torques (Figure 6). We do find significant differences in affected knee joint torques regardless of the symmetry constraints used. Specifically, the experimental data shows knee flexion torques on the affected side during mid-stance, whereas the simulations show no such torques. However, when we compare the muscle forces with experimental EMG [31], [53], [54], we find considerable overlap in the activation timings (Figure 7).

F. Reduced limb mass or limb muscle strength do not affect qualitative gait features

We performed two additional optimizations at various levels of prosthesis work, one with 30% reduced limb mass and one with 30% reduced muscle strength, as recently considered in [31]. These calculations resulted in negligible quantitative differences in torque profiles and joint angle profiles, and small differences in metabolic costs. With the decreased prosthesis mass, we see a slight increase in prosthesis stance time. This trend is qualitatively similar to experiments in which added prosthesis mass tended to decrease prosthesis stance time [40], [55]. We did not observe qualitative differences that suggested that such reduced mass or strength could improve model predictions.

IV. Discussion

In this study, we have presented a computational framework for predicting human walking with a robotic or passive prosthesis and have considered multiple controllers. We have shown that the relationship between prosthesis work and metabolic rate is non-monotonic: the metabolic rate of an amputee first decreases with increasing prosthesis work rate

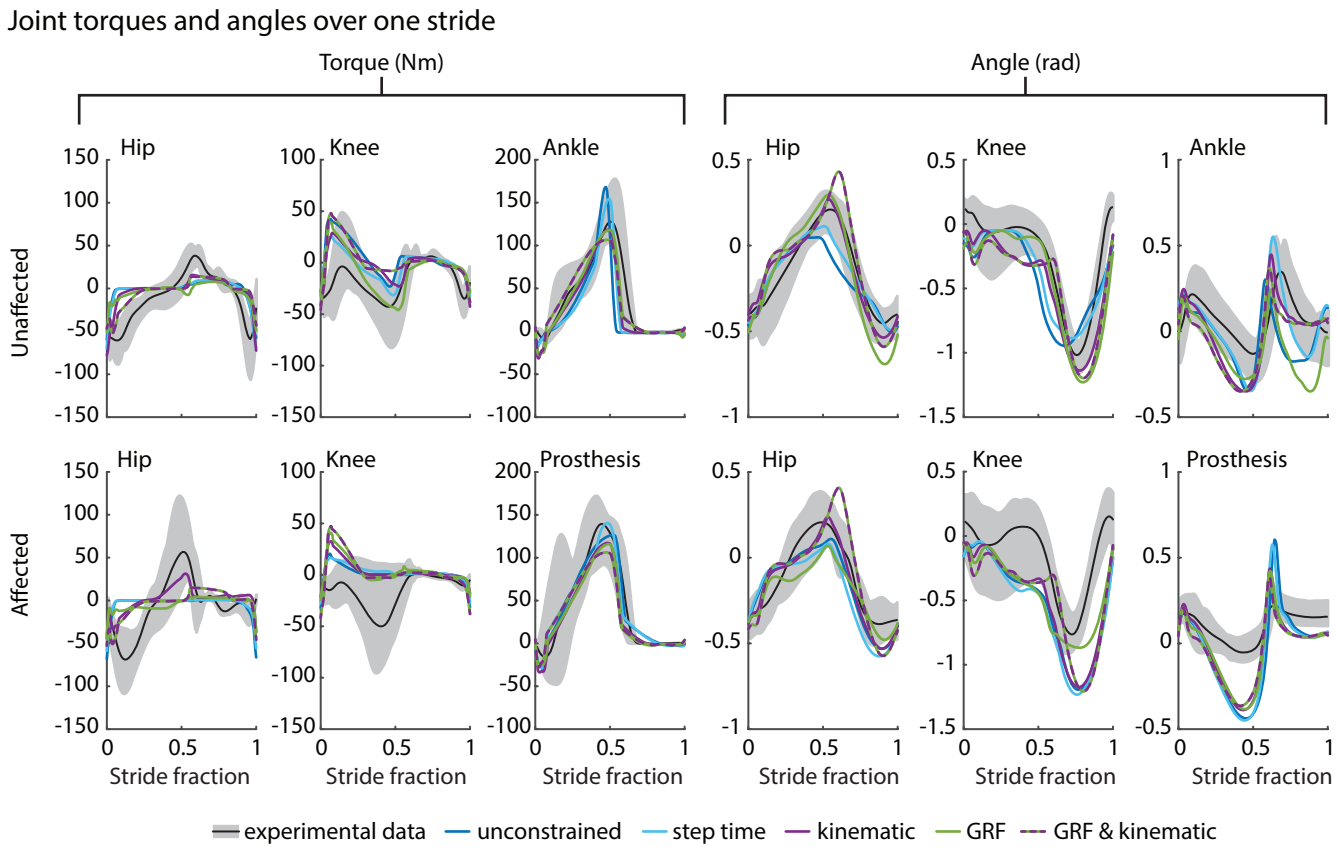

Fig. 6. **Experiment vs model: joint torques and joint angle comparisons with and without symmetry constraints.** This figure presents the joint torques and angles for selected tests (with similar levels of net prosthesis work) using controller 1 with various step time, kinematic, and/or ground reaction force (GRF) symmetry constraints. Results from each symmetry constraint is shown as a separate curve (see legend). Amputee data [5] is overlaid, depicted as a mean curve and 95% confidence interval band (black solid line and gray band). Positive torque and angle values refer to extension and negative refer to flexion; plantarflexion and dorsiflexion are positive and negative respectively for the ankle and prosthesis. Each stride begins with the heel-strike of the corresponding leg being plotted.

and then increases, roughly with a quadratic relationship. This relationship between prosthesis work and metabolic rate was quantitatively similar for all tested controllers. While it is possible that this relationship is common for a wide range of controllers (as suggested by our results), it is also possible that the controllers used here were not sufficiently different from one another in the space of all controllers.

The non-monotonic dependence of metabolic rate with net prosthesis work suggests that simple mechanical-work-based heuristics such as the 'augmentation factor' [56] may not be able to completely capture metabolic reductions at high work rates. Further, augmentation factor (as defined in [56]) may be more appropriate for exoskeletons and not as appropriate for prostheses (without modifications). For instance, we find that the augmentation factor predicts metabolic rate benefit for energy neutral or even energy negative passive prostheses. Nevertheless, the initial slope of the metabolic rate reduction versus work rate is about -4.0, corresponding to the standard 25% efficiency for muscle positive work (Figure 3, see linear term in quadratic fit). This suggests that mechanical-work-based heuristic reasoning [56] may be applicable for smaller work-rates.

Most metabolic measurement studies have shown that amputees experience about 10-30% higher metabolic rate using passive prostheses than their non-amputee control subjects [47], [57]–[59]. Our simulations predict that a SACH foot, which has considerable damping, produces 35% higher metabolic costs than for non-amputees, qualitatively similar to the older experimental studies. When we tested a controller that produces zero net prosthesis work during stance (analogous to a perfect ESR prosthesis with no damping), we found that it is possible to produce non-amputee levels of metabolic rates. Such low metabolic costs seem inconsistent with some older experimental studies. However, the prostheses used in the older experimental studies are not 'zero work' prosthesis. There is always some energy loss in any passive prosthesis, whether it is a SACH foot or an ESR prosthesis like the Flex Foot. The higher costs measured in experiment may also be due to the subjects' physical fitness or training on their prostheses. Indeed, a recent study showed that when physical fitness is not an issue, amputees use about the same metabolic rate as non-amputee control subjects [47], similar to our results from the zero-work-zero-damping condition of the prosthesis controllers. Qualitatively similar conclusions were reached by another recent simulation study [31], albeit by including tracking of normal kinematics in the optimized cost

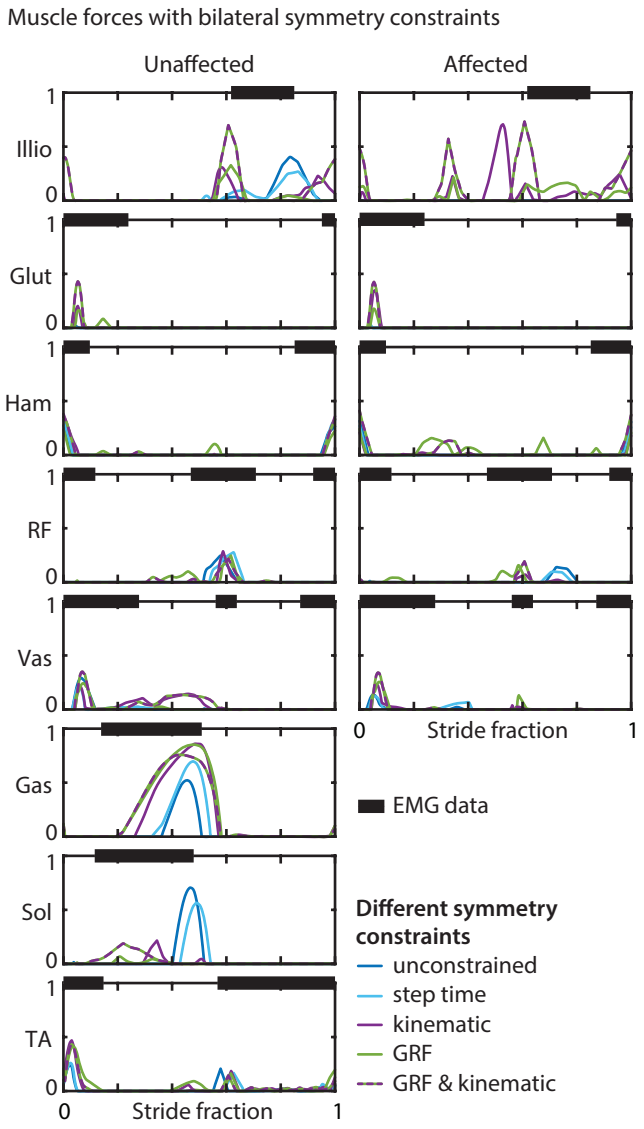

Fig. 7. **Normalized muscle forces with and without symmetry constraints.** Normalized muscle forces are presented over one stride period, as a fraction of maximum isometric force. The curves shown are from optimizations that differ only by the symmetry constraints used (including no symmetry constraints). All optimizations had similar net prosthesis work rate and used prosthesis controller 1. Each stride shown starts from the heel-strike of the leg in which the corresponding muscle is present. Horizontal black bars atop each figure panel are an on/off representation of EMG data taken from experiment [31], [52]–[54].

function.

At net positive prosthesis work rates, we find metabolic rates lower than that of an analogous able-bodied (non-amputee) walking simulation (computed in [32]). Such large metabolic rate reductions do not seem to match those found in experiments thus far. Reductions in metabolic rates in experiment are often small [60], [61] or insignificant [5] and have never produced a metabolic rate below that of a non-amputee.

One source of these large metabolic reductions could be the bilateral asymmetries we see at high work rates in our simulation. In the absence of explicit symmetry constraints, the simulated biped tends to spend more time in stance on the affected side than on the unaffected side (Figure 4), making use of the 'free' power of the prosthesis. When we constrain the biped to walk with equal stance time on each leg, relative metabolic benefit of the high prosthesis work is reduced. If we further constrain the joint angles and/or ground reaction forces to have bilateral symmetry, the metabolic rate increases further and better matches experiment at similar work rates. This suggests that gait symmetry could be a conscious or subconscious goal for the user. So it may be necessary to design prostheses such that the energy optimal gait naturally has high symmetry. This is an open problem. Further, we see that these bilateral symmetry constraints lead to more human like joint torques. For example without any constraints, the push off torque in the unaffected ankle occur more suddenly at the end of stance (Figure 6). By contrast, with constrained kinematic symmetry, the ankle torque ramps up gradually over the stance phase, similar to experiment. Our results here and in a previous study [17], [32] suggest that such improvements in gait symmetry will have a metabolic penalty, but could equalize joint stresses [17], [62]. Based on these results, we speculate that simply implementing the controller inferred from normal human foot function [63]–[66] will still result in substantial gait asymmetry, as the prosthetic ankle will still be an asymmetric source of free propulsive power to the user. We hypothesize that promoting gait symmetry without much metabolic penalty may require augmenting the unilateral prosthesis with an exoskeleton on the unaffected side [56], [67]. We further hypothesize that a human-in-the-loop optimization [67] that systematically moves the gait away from symmetry may produce metabolic reductions greater than those observed so far.

Discrepancies between model-predicted and experimental metabolic rates (Figure 5) could be due to model simplifications, which includes a simplified metabolic model, simplified socket interaction that ignore effects of interfacial forces between the prosthesis and the residual limb [17], simplified ground contact, and perfectly a periodic gait that ignores gait stability. Future work may consider other cost models, such as [68], but to do so would require more complex muscle models which include activation dynamics and force length relationships. Previous work [32] suggested that while using different cost functions resulted in different cost reduction percentages, all cost functions resulted in similar general trends. Similar to discrepancies in metabolic rates, we found that the simulation and data also differed somewhat for kinematics and much more for joint torques (Figure 6). Specifically, our simulations lack knee flexion torques on the affected limb during late stance, but such knee flexion torques are present in the experimental data. This may be due to the walking strategy chosen by the optimization in response to prosthesis controllers with an initial linear spring-like behavior, whereas biological angle torque-angle loops can be more nonlinear. As shown in Figure 6, the simulated knee is flexed during late stance, so a flexion torque (which can only be produced by the biarticular hamstring) would cause the knee to collapse further rather than just extend the hip (as it would if the knee was locked). Another possibility is that, in our model, the unaffected side does not have a residual gastrocnemius, which

can have some activity in transtibial amputees, resulting in knee flexion moments [69], [70].

Given that detailed quantitative agreement between model predictions and walking data (without any fitting) is an open problem, our goal here was to mainly establish qualitative predictions for humans walking with robotic prostheses similar to past non-amputee simulations [14], [15]. Past work on even non-amputee models also contained large errors in predicted forces and torques and smaller errors in predicted kinematics [15]. It has been possible to obtain better agreement between model and data using explicit fitting to experimental data [14], [31], but even then, the kinematic match has been better than the kinetic (force) match.

One possible interpretation of our results is as a negative result: that is, that amputees do not walk in a manner that just minimizes metabolic rate, subject to the above caveats about model simplicity. For instance, amputees may artificially co-contract to improve stability [71]–[73], increasing metabolic expenditure while keeping mechanical work similar. Amputee walking may also be adapted to reduce affected limb joint loading, socket loading, or more generally, increase comfort and reduce pain. So, in future work, we will consider adding such loading terms as part of the objective to be minimized (e.g., [17], [74]).

Amputees are known to have reduced muscle strength on the affected side [75]–[77], an aspect we have mostly ignored in our modeling here except for a few optimization calculations with reduced maximum isometric force. The effects of retaining muscle strength was considered in more detail in a recent simulation study [31]. The gait optimizations in that simulation study [31] had an objective to track normal kinematics in addition to a metabolic rate term. They found that reduction of muscle strength resulted in increased metabolic rate, whereas retaining normal muscle strength resulted in a normal metabolic rate.

Our model of the human sensorimotor system has been particularly simple: we assumed that the human motor system will eventually converge to the metabolic minimum, as humans are known to do in the presence of prostheses [24] or exoskeletons [26], [67]. By focusing exclusively on metabolic rate, we have ignored the active feedback control by the human sensorimotor system. This active feedback control can be in the form of fast reflexes or longer latency feedback control. Inclusion of such human motor control would be desirable in our simulation, as that would further constrain the space of possible muscle activations and walking strategies. Unfortunately, we do not yet have a good enough characterization of the human walking sensorimotor system at the level of each muscle. For instance, Geyer and colleagues [61], [78] have proposed a reflex-based controller for walking that has been used both for prosthesis control [61] and as a hypothesis of human motor control [78]. But the detailed structure and parameters of such feedback controller models have not been validated using joint-level or muscle-level human experiments. Nevertheless, constraining our optimizations by such simple models of human motor control may provide valuable insight into the qualitative effect of such control. At least in the short time-scale, when the amputee has had only limited practice with the prosthesis, it is conceivable that the human motor control system treats the active power from a robotic prosthesis as a 'perturbation' to be rejected, rather than 'assistance' to be taken advantage of. One subtlety in modeling the amputee motor control system is that the amputated limb is not an explicit part of the human sensorimotor loop. For instance, the human nervous system does not have direct sensory information of the prosthesis state and torque. However, it is known that humans can adapt to forceful interactions with exoskeletons whose internal state are not directly accessible to the user [26], [67].

In future work, we will model the prosthesis morphology and controller used in specific experiments [2], [5] with greater fidelity, so that a better comparison may be made. For instance, the prosthesis emulator in [2], [5] is designed with a separated toe (actuated) and heel (passive), whereas the simulated prosthesis is a single rigid body. We can also model the socket with greater fidelity as our current model assumes that the prosthesis is rigidly attached to the leg. Amputees, however, interface with their prosthesis through a socket system. Forces are transferred from prosthesis to the rest of the body through soft tissues, which could be modeled as a three degree of freedom socket joint. We may also wish to consider a wider range of walking behavior, for instance, walking at different speeds, at different slopes, with accelerations and decelerations including starting and stopping, or with changing directions (turning using a 3D model).

We have focused here on unilateral prosthesis with a specific class of feedback controllers. We could apply the same techniques to obtain predictions about a broad class of prosthesis and exoskeleton controllers, including those that rely on other human body and myoelectric state variables [79], qualitatively inspired by neuromuscular control [61], or to explore and optimize the effect of geometry of the prosthesis [80]. The long-term goal is a general framework for model-based rational design of biomechatronic devices. Our approach can test high dimensional device controllers with thousands of parameters, and could, therefore, be a complement to the human-in-the-loop optimization approaches, which are usually constrained to exploring low-dimensional search spaces.

V. Acknowledgment

This work was supported by NSF CMMI grants 1300655 and 1254842. The authors thank Steve Collins and Joshua Caputo for discussions informing this research.

References

[1] L. Torburn, J. Perry, E. Ayyappa, and S. L. Shanfield, "Below-knee amputee gait with dynamic elastic response prosthetic feet: a pilot study.," *J. Rehabil. Res. Dev.*, vol. 27, p. 369, 1990.

[2] J. Caputo and S. Collins, "A universal ankle-foot prosthesis emulator for human locomotion experiments'," *J. Biomech. Eng.*, vol. 136, p. 035002, 2014.

[3] H. Herr and A. Grabowski, "Bionic ankle-foot prosthesis normalizes walking gait for persons with leg amputation," *Proc. R. Soc. B*, vol. 279, pp. 457–464, 2012.

[4] S. Au, J. Weber, and H. Herr, "Powered ankle-foot prosthesis improves walking metabolic economy," *IEEE Trans. Robot.*, vol. 25, pp. 51–66, 2009.

[5] R. E. Quesada, J. M. Caputo, and S. H. Collins, "Increasing ankle push-off work with a powered prosthesis does not necessarily reduce metabolic rate for transtibial amputees," *J. Biomech.*, vol. 49, pp. 3452–3459, 2016.

[6] J. M. Caputo, P. G. Adamczyk, and S. H. Collins, "Informing ankle-foot prosthesis prescription through haptic emulation of candidate devices," in *Proc. IEEE Int. Conf. Robot. Autom.*, pp. 6445–6450, 2015.

[7] A. Hessel, U. Tahir, J. Petak, R. Lemoyne, J. Tester, and K. Nishikawa, "A powered ankle-foot prosthesis with a neuromuscular based control algorithm can successfully mimic human walking.," in *Integr. Comp. Biol.*, vol. 55, pp. E274–E274, 2015.

[8] P. A. Bhounsule, J. Cortell, A. Grewal, B. Hendriksen, J. G. D. Karssen, C. Paul, and A. Ruina, "Low-bandwidth reflex-based control for lower power walking: 65 km on a single battery charge," *Int. J. Robot. Res*, vol. 33, pp. 1305–1321, 2014.

[9] M. Kim and S. H. Collins, "Once-per-step control of ankle-foot prosthesis push-off work reduces effort associated with balance during human walking," *J. Neuroeng. Rehabil.*, vol. 12, p. 43, 2015.

[10] J. M. Caputo, *Informing ankle-foot prosthesis design and prescription through systematic experimentation with a tethered robotic prosthesis*. PhD thesis, Carnegie Mellon University Pittsburgh, PA, 2015.

[11] W. Felt, J. C. Selinger, J. M. Donelan, and C. D. Remy, "Body-in-the-loop: Optimizing device parameters using measures of instantaneous energetic cost," *PloS One*, vol. 10, p. e0135342, 2015.

[12] J. L. Contreras-Vidal, A. Kilicarslan, H. Huang, and R. G. Grossman, "Human-centered design of wearable neuroprostheses and exoskeletons," *AI Magazine*, vol. 36, pp. 12–22, 2015.

[13] Y. Wen, J. Si, X. Gao, S. Huang, and H. H. Huang, "A new powered lower limb prosthesis control framework based on adaptive dynamic programming," *IEEE Trans. Neural Netw.*, vol. 28, pp. 2215 – 2220, 2017.

[14] R. H. Miller, "A comparison of muscle energy models for simulating human walking in three dimensions," *J. Biomech.*, vol. 47, pp. 1373–1381, 2014.

[15] M. Ackermann and A. J. van den Bogert, "Optimality principles for model-based prediction of human gait," *J. Biomech.*, vol. 43, pp. 1055–1060, 2010.

[16] A. E. Martin and J. P. Schmiedeler, "Predicting healthy human and amputee walking gait using ideas from underactuated robot control," in *ICRA Workshop on Human Modeling and Control for Assistive Technologies*, 2014.

[17] A. D. Koelewijn and A. J. van den Bogert, "Joint contact forces can be reduced by improving joint moment symmetry in below-knee amputee gait simulations," *Gait Posture*, vol. 49, pp. 219–225, 2016.

[18] V. Joshi and M. Srinivasan, "Walking on a moving surface: energy-optimal walking motions on a shaky bridge and a shaking treadmill can reduce energy costs below normal," *Proc. R. Soc. A*, vol. 471, p. 20140662, 2015.

[19] J. M. Donelan, R. Kram, *et al.*, "Mechanical and metabolic determinants of the preferred step width in human walking," *Proc. Roy. Soc. B*, vol. 268, pp. 1985–1992, 2001.

[20] A. Minetti and R. Alexander, "A theory of metabolic costs for bipedal gaits," *J. Theor. Biol*, vol. 186, pp. 467–476, 1997.

[21] M. Srinivasan, "Fifteen observations on the structure of energy minimizing gaits in many simple biped models," *J. R. Soc. Interface*, vol. 8, pp. 74–98, 2011.

[22] M. Handford and M. Srinivasan, "Sideways walking: preferred is slow, slow is optimal, and optimal is expensive," *Biol. Lett.*, vol. 10, p. 20131006, 2014.

[23] L. L. Long and M. Srinivasan, "Walking, running, and resting under time, distance, and average speed constraints: optimality of walk–run–rest mixtures," *J. Roy. Soc. Interface*, vol. 10, p. 20120980, 2013.

[24] H. Ralston, "Energy-speed relation and optimal speed during level walking," *Int. Z. Angew Physiol.*, vol. 17, pp. 277–283, 1958.

[25] N. Seethapathi and M. Srinivasan, "The metabolic cost of changing walking speeds is significant, implies lower optimal speeds for shorter distances, and increases daily energy estimates," *Biol. Lett.*, vol. 11, p. 20150486, 2015.

[26] J. C. Selinger, S. M. O'Connor, J. D. Wong, and J. M. Donelan, "Humans can continuously optimize energetic cost during walking," *Curr. Biol.*, vol. 25, pp. 2452–2456, 2015.

[27] J. M. Finley, A. J. Bastian, and J. S. Gottschall, "Learning to be economical: the energy cost of walking tracks motor adaptation," *J. Physiol.*, vol. 591, pp. 1081–1095, 2013.

[28] A. LaPre, B. Umberger, and F. Sup, "Simulation of a powered ankle prosthesis with dynamic joint alignment," in *Conf. Proc. IEEE Eng. Med. Biol. Soc.*, pp. 1618–1621, 2014.

[29] N. T. Pickle, J. M. Wilken, J. M. Aldridge, R. R. Neptune, and A. K. Silverman, "Whole-body angular momentum during stair walking using passive and powered lower-limb prostheses," *J. Biomech.*, vol. 47, pp. 3380–3389, 2014.

[30] H. Zhao, J. Reher, J. Horn, V. Paredes, and A. D. Ames, "Realization of nonlinear real-time optimization based controllers on self-contained transfemoral prosthesis," in *Proc. ACM/IEEE 6th Int. Conf. Cyber-Physical Systems*, pp. 130–138, ACM, 2015.

[31] E. R. Esposito and R. H. Miller, "Maintenance of muscle strength retains a normal metabolic cost in simulated walking after transtibial limb loss," *PloS One*, vol. 13, p. e0191310, 2018.

[32] M. Handford and M. Srinivasan, "Robotic lower limb prosthesis design through simultaneous computer optimizations of human and prosthesis costs," *Sci. Rep.*, vol. 6, 2016.

[33] A. H. Hansen, D. S. Childress, S. C. Miff, S. A. Gard, and K. P. Mesplay, "The human ankle during walking: implications for design of biomimetic ankle prostheses," *J. Biomech.*, vol. 37, pp. 1467–1474, 2004.

[34] F. Sup, A. Bohara, and M. Goldfarb, "Design and control of a powered transfemoral prosthesis," *Int. J. Robot. Res.*, vol. 27, pp. 263–273, 2008.

[35] K. Shamaei, G. S. Sawicki, and A. M. Dollar, "Estimation of quasi-stiffness and propulsive work of the human ankle in the stance phase of walking," *PloS One*, vol. 8, p. e59935, 2013.

[36] F. E. Zajac, "Muscle and tendon properties models scaling and application to biomechanics and motor," *Critical reviews in biomedical engineering*, vol. 17, pp. 359–411, 1989.

[37] K. Gerritsen, A. van den Bogert, M. Hulliger, and R. Zernicke, "Intrinsic muscle properties facilitate locomotor control - a computer simulation study," *Motor Control*, vol. 2, pp. 206–220, 1998.

[38] A. Van den Bogert, "Gait2de – a musculoskeletal dynamics model for posture and gait," in *Conf. on Dynamic Walking, Jena*, 2011.

[39] A. E. Ferris, J. D. Smith, G. D. Heise, R. N. Hinrichs, and P. E. Martin, "A general model for estimating lower extremity inertial properties of individuals with transtibial amputation," *J. Biomech.*, vol. 54, pp. 44–48, 2017.

[40] S. Mattes, P. E. Martin, and T. Royer, "Walking symmetry and energy cost in persons with unilateral transtibial amputations: matching prosthetic and intact limb inertial properties," *Arch Phys Med Rehabil.*, vol. 81, pp. 561–568, 2000.

[41] S.-J. Lin-Chan, D. H. Nielsen, H. J. Yack, M.-J. Hsu, and D. G. Shurr, "The effects of added prosthetic mass on physiologic responses and stride frequency during multiple speeds of walking in persons with transtibial amputation1," *Arch. Phys. Med. Rehabil.*, vol. 84, pp. 1865–1871, 2003.

[42] R. W. Selles, J. B. Bussmann, R. C. Wagenaar, and H. J. Stam, "Effects of prosthetic mass and mass distribution on kinematics and energetics of prosthetic gait: a systematic review," *Arch. Phys. Med. Rehabil.*, vol. 80, pp. 1593–1599, 1999.

[43] J. T. Betts, *Practical methods for optimal control and estimation using nonlinear programming*, vol. 19. SIAM, 2010.

[44] P. E. Gill, W. Murray, and M. A. Saunders, "Snopt: An sqp algorithm for large-scale constrained optimization," *SIAM review*, vol. 47, pp. 99–131, 2005.

[45] M. Srinivasan, "Optimal speeds for walking and running, and walking on a moving walkway," *Chaos*, vol. 19, p. 026112, 2009.

[46] J. Doke and A. D. Kuo, "Energetic cost of producing cyclic muscle force, rather than work, to swing the human leg," *J. Exp. Biol.*, vol. 210, pp. 2390–2398, 2007.

[47] E. R. Esposito, K. M. Rodriguez, C. A. Ràbago, and J. M. Wilken, "Does unilateral transtibial amputation lead to greater metabolic demand during walking?," *J. Rehabil. Res. Dev.*, vol. 51, pp. 1287–1296, 2014.

[48] R. Alexander, "Three uses for springs in legged locomotion," *Int. J. Robotics Res.*, vol. 9, pp. 53–61, 1990.

[49] S. H. Collins, M. B. Wiggin, and G. S. Sawicki, "Reducing the energy cost of human walking using an unpowered exoskeleton," *Nature*, vol. 522, p. 212, 2015.

[50] H. Geyer, A. Seyfarth, and R. Blickhan, "Compliant leg behaviour explains basic dynamics of walking and running," *Proc. Roy. Soc. B: Biol. Sci.*, vol. 273, pp. 2861–2867, 2006.

[51] J. Dingwell, B. Davis, and D. Frazder, "Use of an instrumented treadmill for real-time gait symmetry evaluation and feedback in normal and transtibial amputee subjects," *Prosthet. Orthot. Int.*, vol. 20, pp. 101–110, 1996.

[52] D. A. Winter and S. E. Sienko, "Biomechanics of below-knee amputee gait," *J. Biomech.*, vol. 21, pp. 361–367, 1988.

[53] D. H. Sutherland, "The evolution of clinical gait analysis part l: kinesiological emg," *Gait Posture*, vol. 14, pp. 61–70, 2001.

[54] R. L. Cromwell, T. K. Aadland-Monahan, A. T. Nelson, S. M. Stern-Sylvestre, and B. Seder, "Sagittal plane analysis of head, neck, and trunk kinematics and electromyographic activity during locomotion," *J. Orthop. Sports Phys. Ther.*, vol. 31, pp. 255–262, 2001.

[55] J. D. Smith and P. E. Martin, "Effects of prosthetic mass distribution on metabolic costs and walking symmetry," *Journal of Applied Biomechanics*, vol. 29, pp. 317–328, 2013.
[56] L. M. Mooney, E. J. Rouse, and H. M. Herr, "Autonomous exoskeleton reduces metabolic cost of human walking," *J. Neuroeng. Rehabil.*, vol. 11, p. 151, 2014.
[57] R. S. Gailey, M. S. Nash, T. A. Atchley, R. M. Zilmer, G. R. Moline-Little, N. Morris-Cresswell, and L. I. Siebert, "The effects of prosthesis mass on metabolic cost of ambulation in non-vascular trans-tibial amputees," *Prosthet. Orthot. Int.*, vol. 21, pp. 9–16, 1997.
[58] J. J. Genin, G. J. Bastien, B. Franck, C. Detrembleur, and P. A. Willems, "Effect of speed on the energy cost of walking in unilateral traumatic lower limb amputees," *Eur. J. Appl. Physiol.*, vol. 103, p. 655, 2008.
[59] N. Molen, "Energy/speed relation of below-knee amputees walking on a motor-driven treadmill," *Eur. J. Appl. Physiol.*, vol. 31, pp. 173–185, 1973.
[60] J. Caputo and S. Collins, "Prosthetic ankle push-off work reduces metabolic rate but not collision work in non-amputee walking," *Sci. Rep.*, vol. 4, pp. 51–66, 2014.
[61] M. Eilenberg, H. Geyer, and H. Herr, "Control of a powered ankle-foot prosthesis based on a neuromuscular model," *IEEE Trans. Neural Syst. Rehabil. Eng*, vol. 18, pp. 164–173, 2010.
[62] A. E. Martin, *Predictive modeling of healthy and amputee walking using a simple planar model*. University of Notre Dame, 2014.
[63] E. J. Rouse, L. J. Hargrove, E. J. Perreault, and T. A. Kuiken, "Estimation of human ankle impedance during the stance phase of walking," *IEEE Trans. Neural Syst. Rehabil. Eng.*, vol. 22, pp. 870–878, 2014.
[64] G. S. Sawicki and D. P. Ferris, "Powered ankle exoskeletons reveal the metabolic cost of plantar flexor mechanical work during walking with longer steps at constant step frequency," *J. Exp. Biol.*, vol. 212, pp. 21–31, 2009.
[65] H. Lee and N. Hogan, "Time-varying ankle mechanical impedance during human locomotion," *IEEE Trans. Neural Syst. Rehabil. Eng.*, vol. 23, pp. 755–764, 2015.
[66] Y. Wang and M. Srinivasan, "Stepping in the direction of the fall: the next foot placement can be predicted from current upper body state in steady-state walking," *Biol. Lett.*, vol. 10, p. 20140405, 2014.
[67] J. Zhang, P. Fiers, K. A. Witte, R. W. Jackson, K. L. Poggensee, C. G. Atkeson, and S. H. Collins, "Human-in-the-loop optimization of exoskeleton assistance during walking," *Science*, vol. 356, pp. 1280–1284, 2017.
[68] B. R. Umberger, "Stance and swing phase costs in human walking," *J. Roy. Soc. Interface*, vol. 7, pp. 1329–1340, 2010.
[69] S. Huang and D. P. Ferris, "Muscle activation patterns during walking from transtibial amputees recorded within the residual limb-prosthetic interface," *J. Neuroeng. Rehabil.*, vol. 9, p. 55, 2012.
[70] B. Silver-Thorn, T. Current, and B. Kuhse, "Preliminary investigation of residual limb plantarflexion and dorsiflexion muscle activity during treadmill walking for trans-tibial amputees," *Prosthetics and orthotics international*, vol. 36, pp. 435–442, 2012.
[71] S. Hirokawa, M. Solomonow, Z. Luo, Y. Lu, and R. D'ambrosia, "Muscular co-contraction and control of knee stability," *J. Electromyogr. Kinesiol.*, vol. 1, pp. 199–208, 1991.
[72] N. Hogan, "Adaptive control of mechanical impedance by coactivation of antagonist muscles," *IEEE Trans. Automat. Contr.*, vol. 29, pp. 681–690, 1984.
[73] M. Seyedali, J. M. Czerniecki, D. C. Morgenroth, and M. E. Hahn, "Co-contraction patterns of trans-tibial amputee ankle and knee musculature during gait," *J. Neuroeng. Rehabil.*, vol. 9, p. 29, 2012.
[74] R. H. Miller, S. C. Brandon, and K. J. Deluzio, "Predicting sagittal plane biomechanics that minimize the axial knee joint contact force during walking," *J. Biomech. Eng.*, vol. 135, p. 011007, 2013.
[75] E. Isakov, H. Burger, M. Gregorič, and C. Marinček, "Isokinetic and isometric strength of the thigh muscles in below-knee amputees," *Clin. Biomech.*, vol. 11, pp. 233–235, 1996.
[76] A. Pedrinelli, M. Saito, R. Coelho, R. Fontes, and R. Guarniero, "Comparative study of the strength of the flexor and extensor muscles of the knee through isokinetic evaluation in normal subjects and patients subjected to trans-tibial amputation," *Prosthet. Orthot. Int.*, vol. 26, pp. 195–205, 2002.
[77] E. Isakov, H. Burger, M. Gregorič, and Č. Marinčcek, "Stump length as related to atrophy and strength of the thigh muscles in trans-tibial amputees," *Prosthet. Orthot. Int.*, vol. 20, pp. 96–100, 1996.
[78] H. Geyer and H. Herr, "A muscle-reflex model that encodes principles of legged mechanics produces human walking dynamics and muscle activities," *IEEE Trans. Neural. Syst. Rehabil. Eng.*, vol. 18, pp. 263–273, 2010.
[79] D. P. Ferris, K. E. Gordon, G. S. Sawicki, and A. Peethambaran, "An improved powered ankle–foot orthosis using proportional myoelectric control," *Gait Posture*, vol. 23, pp. 425–428, 2006.
[80] S. Pfeifer, R. Riener, and H. Vallery, "An actuated transfemoral prosthesis with optimized polycentric knee joint," in *IEEE Int. Conf. Biomedical Robotics and Biomechatronics (BioRob)*, pp. 1807–1812, IEEE, 2012.